LINEAR PARAMETER VARYING CONTROLLERS FOR FLEXIBLE ROTORS SUPPORTED ON MAGNETIC BEARINGS

Stephen Mason,[1,*] Panagiotis Tsiotras,[1] Paul Allaire[1]

ABSTRACT

In this paper we provide a methodology for designing Linear Parameter Varying (LPV) controllers for use with magnetic bearings for flexible high-speed rotors in rotating machinery applications. The dependence of the gyroscopic and imbalance forces on the rotational speed of the rotor, combined with the ability to measure speed in real time, motivates the need for a controller which is scheduled on the rotational speed. The LPV method for computing a controller, which ensures stability and bounds on performance for all speeds within a given speed range, is used. Simulations are presented which compare the effectiveness of LPV controllers to a set of single-speed, gain-scheduled, optimal $\mathcal{H}_\infty$ controllers.

INTRODUCTION

The modeling and control of flexible rotating machinery with imbalance becomes increasingly complicated when large changes in operating speed are expected. This problem is made worse by gyroscopic effects, due to the speed-dependent coupling along the transverse rotor axes. Imbalances impose synchronous forces with the rotational speed, whose magnitudes are proportional to the square of the speed. With such a dependence on a system parameter, which may vary greatly, it is important that a given controller be able to handle the plant changes with rotational speed. Rotor flexibility effects worsen the control problem as the natural frequencies of the rotor also change with the rotor speed. To address this problem, gain-scheduled robust controller synthesis techniques have been used in the past (Sivrioglu and Nonami 1996, Matsumura *et al.* 1996).

In this paper we apply the theory of self-scheduled $\mathcal{H}_\infty$ control theory as developed recently in (Apkarian *et al.* 1994, Apkarian *et al.* 1995, Apkarian and Gahinet 1995, Packard 1994) to control a flexible shaft supported on magnetic bearings. The rotor system exhibits significant gyroscopics and imbalance forces. First, we develop a linearly, parameter varying (LPV) state-space description of the rotor model with respect to the rotor speed. Using the results of (Apkarian and Gahinet 1995) we design a self-scheduled $\mathcal{H}_\infty$ controller for this LPV system. Numerical simulations compare the performance of this LPV controller with a series of gain-scheduled, single-speed $\mathcal{H}_\infty$ controllers.

*Currently at Applied Physics Lab, Johns Hopkins University, Laurel, MD 20723, USA.

[1]Department of Mechanical, Aerospace and Nuclear Engineering, University of Virginia, Charlottesville, VA 22903-2442, USA.

System Model

In this section we present the main elements of the system used in this work. For a more detailed exposition the interested reader may consult (Mason 1997).

Flexible rotor model

At the Center for Magnetic Bearings at the University of Virginia a test rig is under construction to test modern control algorithms for gyroscopic and unbalanced rotating machinery supported on active magnetic bearings. This test rig is shown in Fig. 1 in a horizontal configuration. During operation, the shaft is located vertically and it is approximately 0.864 m (34 in) in length. Three magnetic actuator disks are located on the shaft. The lower and upper disks (items 2 and 5 in Fig. 1) are used as regular bearings. The middle disk (item 3 in Fig. 1) can be used to impose disturbances on the rotor. Sensors measuring displacements of the shaft are located at the middle and upper disks, as well as at the midspan disk. The operating speed range considered here is 104 rad/sec to 832 rad/sec (1,000 to 8,000 rpm).

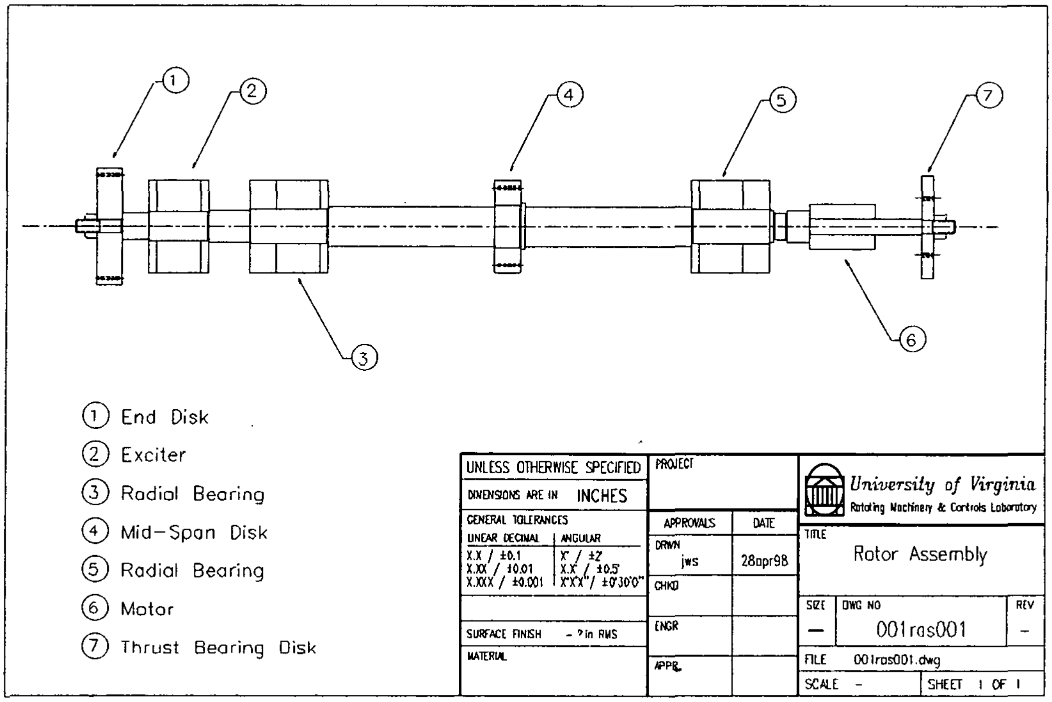

Figure 1: The test rig.

The equations for a flexible rotor can be derived using a finite element approach (Ahrens *et al.* 1996), (Nonami and Ito 1996), (Maslen and Allaire 1991). The program MODAL developed at the University of Virginia uses this method to generate a linear, speed-dependent state-space model incorporating flexibility and gyroscopic affects. The state-space model of the flexible shaft is of the form

$$\frac{d}{dt}\left\{\begin{array}{c}\underline{m}_X\\ \underline{m}_Y\end{array}\right\}=\left[\begin{array}{cc}A_m & -pG_m\\ pG_m & A_m\end{array}\right]\left\{\begin{array}{c}\underline{m}_X\\ \underline{m}_Y\end{array}\right\}+\left[\begin{array}{cc}B_m & 0\\ 0 & B_m\end{array}\right]\left\{\begin{array}{c}\mathbf{f}_X\\ \mathbf{f}_Y\end{array}\right\}, \tag{1}$$

$$\left\{ \begin{array}{c} \mathbf{r}_X \\ \mathbf{r}_Y \end{array} \right\} = \left[\begin{array}{cc} C_m & 0 \\ 0 & C_m \end{array} \right] \left\{ \begin{array}{c} \underline{m}_X \\ \underline{m}_Y \end{array} \right\}. \tag{2}$$

where $\underline{m}_X$ and $\underline{m}_Y$ denote the vectors of modal states (mode shapes) in the X and Y directions, respectively. The inputs $\mathbf{f}_X$ and $\mathbf{f}_Y$ are forces in X and Y directions specified at particular mass stations, and the outputs $\mathbf{r}_X$ and $\mathbf{r}_Y$ are displacements at certain mass stations of concern.

In (1), p is the rotational speed of the rotor. Gyroscopics act as a cross coupling between motion in the X and Y directions due to the rotor speed and is manifested by the gyroscopic matrix G_m in (1). We can write (1) and (2) compactly as

$$\begin{aligned} \dot{\mathbf{M}} &= A(p)\mathbf{M} + B\mathbf{F} \\ \mathbf{R} &= C\mathbf{M} \end{aligned} \tag{3}$$

with

$$\mathbf{M} = \left\{ \begin{array}{c} \underline{m}_X \\ \underline{m}_Y \end{array} \right\}, \quad \mathbf{F} = \left\{ \begin{array}{c} \mathbf{f}_X \\ \mathbf{f}_Y \end{array} \right\}, \quad \mathbf{R} = \left\{ \begin{array}{c} \mathbf{r}_X \\ \mathbf{r}_Y \end{array} \right\} \tag{4}$$

$$A(p) = \left[\begin{array}{cc} A_m & -p\,G_m \\ p\,G_m & A_m \end{array} \right], \quad B = \left[\begin{array}{cc} B_m & 0 \\ 0 & B_m \end{array} \right], \quad C = \left[\begin{array}{cc} C_m & 0 \\ 0 & C_m \end{array} \right]. \tag{5}$$

For each retained rigid or flexible mode, the model contains 4 states: The modal state itself, in the X and Y direction, and its first derivative in the X and Y direction. It should be noted that this model does not contain acceleration ($\dot{p}$) terms and, thus, is not necessarily accurate for rapid changes in rotational speed. For a more detailed discussion on the derivation of (3) one may consult (Mason 1997).

Bearing forces

The force acting on a rotor due to an electromagnetic bearing can be expressed by a simple, linearized model incorporating a current stiffness, K_i, and a displacement stiffness, K_x (Maslen and Allaire 1991). The force acting on the rotor in, say, the X direction due to any one magnet is given by

$$f_{bx} = K_i(i - i_o) - K_x(x - x_o) \tag{6}$$

where i_o is some nominal bias current and x_o is a nominal displacement. We let the control effort at this magnet, u, be defined as $i - i_o$, the deviation of the current from the bias value. We define the measured displacement x as the displacement from the center axis, so that $x_o = 0$. The force equation then becomes

$$f_{bx} = K_i u - K_x x. \tag{7}$$

It is assumed that a deviation from the bias value on one side of the bearing is matched with an equal but opposite deviation on the other side.

The influence of a force f_{bx} on a given modal state $\mathbf{M}_n$ is given next. Taking one row from (3) corresponding to the magnetic bearing location and substituting the expression for f_{bx} given in (7) one obtains

$$\dot{\mathbf{M}}_n = A_n\mathbf{M} - B_b K_x x_n + B_b K_i u \tag{8}$$

where A_n is the nth row of the A matrix and B_b is the element of B on the nth row in the column associated with the bearing force input f_{bx}. The displacement x_n is the displacement at the magnet in question, given by $x_n = C_b\mathbf{M}$, where C_b is the row of C associated with the displacement at the bearing. Substituting x_n in (8) gives

$$\dot{\mathbf{M}}_n = (A_n - B_b K_x C_b)\mathbf{M} + B_b K_i u. \tag{9}$$

Equation (9) can be expressed as

$$\dot{\mathbf{M}}_n = \hat{A}_n \mathbf{M} + \hat{B}_n u \tag{10}$$

with $\hat{A}_n = A_n - B_b K_x C_b$ and $\hat{B}_n = B_b K_i$. The new rotor dynamics model, incorporating the magnetic bearings, is then

$$\begin{aligned} \dot{\mathbf{M}} &= \hat{A}\mathbf{M} + \hat{B}\mathbf{u} \\ \mathbf{R} &= C\mathbf{M} \end{aligned} \tag{11}$$

where $\hat{A}$ and $\hat{B}$ are the matrices formed from the rows $\hat{A}_n$ and $\hat{B}_n$, after accounting for all of the bearings. The inputs $\mathbf{u} = (u_1, u_2, u_3, u_4)$ are the control inputs to the bearings (deviations in current from the bias value), and the outputs are displacements at the sensor locations.

Imbalance forces

In this study imbalance forces are modeled as exogenous disturbance forces acting on the rotor. The controller attempts to minimize the effect of these imbalance forces on the forces at the bearings. One drawback of this approach is that one must assume a particular location at which these imbalance forces are applied, information that may not be readily available. However, in practice, certain portions of a rotor are more susceptible to imbalance than others (places where a large disk, fan, or motor are located, for instance). In such cases it is reasonable to have the controller concentrate on these locations.

The imbalance forces f_{ix} and f_{iy} are typically given by

$$\begin{aligned} f_{ix} &= p^2 \cos(pt)\tilde{d} \\ f_{iy} &= p^2 \sin(pt)\tilde{d} \end{aligned} \tag{12}$$

where p is the rotational speed of the rotor and $\tilde{d}$ is some constant, accounting for the magnitude of the imbalance.

In this investigation, we are more concerned with how the system responds to a given imbalance force at a certain speed than with accurately modeling the changes in imbalance magnitude over the range of operating speed. To easily compare the response over all speeds, it makes sense to keep the magnitude of the imbalance forces constant. Because the forces are generated by a magnetic actuator, which we can control, rather than an actual imbalance weight, this approach presents no difficulties from an experimental standpoint. Ultimately, we will need to include a p^2 imbalance model, because the rotor will have some amount of mechanical imbalance. This can be easily accomplished as shown in (Mason 1997). For now, however, we drop the p^2 dependence from the force equations (12), and write the state-space subsystem as in (13)

$$\dot{\mathbf{x}}_i = \begin{bmatrix} 0 & -p \\ p & 0 \end{bmatrix} \mathbf{x}_i + \begin{bmatrix} 1 \\ 0 \end{bmatrix} \tilde{d} \qquad y_i = \begin{bmatrix} 1 & 0 \\ 0 & 1 \end{bmatrix} \mathbf{x}_i \tag{13}$$

Repeating the process for the Y plane as well, the imbalance forces are thereby incorporated into an augmented model which is of the form

$$\begin{aligned} \dot{x} &= A(p)x + B_1 w + B_2 u \\ z &= C_1 x + D_{12} u \\ y &= C_2 x + D_{21} w \end{aligned} \tag{14}$$

The inputs of this system are the "disturbance signal" $w = \tilde{d}$ and control currents $u = \mathbf{u}$, and its outputs y are displacements at the sensor locations. The performance variable z, to be defined later, includes shaft displacement, transmission of forces to the frame, and excessive control effort.

Self-scheduled LPV controllers

In this paper we use the methodology of (Apkarian *et al.* 1995) and (Apkarian and Gahinet 1995) in order to design self-scheduled controllers (with respect to the parameter p) for the magnetic bearing system described by (14). To this end, consider (polytopic) LPV systems of the form

$$\begin{aligned} \dot{x} &= A(p)x + B_1(p)w + B_2(p)u \\ z &= C_1(p)x + D_{11}(p)w + D_{12}(p)u \\ y &= C_2(p)x + D_{21}(p)w + D_{22}(p)u \end{aligned} \tag{15}$$

The system matrices are assumed to belong to the polytope $\mathcal{S}$ defined by

$$\mathcal{S} := \mathrm{Co}\left\{ \begin{pmatrix} A_i & B_{1i} & B_{2i} \\ C_{1i} & D_{11i} & D_{12i} \\ C_{2i} & D_{21i} & D_{22i} \end{pmatrix}, i = 1, ..., r \right\} \tag{16}$$

where $A_i, B_{1i}, ...,$ denote the values of the matrices $A(p), B_1(p), ...$ at the vertices $\hat{p}_i$ of the parameter polytope $\mathcal{P}$. Henceforth we will assume that in Eqs. (15) the system matrices $B_2(p), C_2(p), D_{12}(p)$ and $D_{21}(p)$ are parameter-independent. In addition, the disturbance does not affect the performance output and there is no feedthrough term from the input to the measured output, i.e., $D_{11}(p) = D_{22}(p) = 0$. These simplifying assumptions can be relaxed, at the expense of increased complexity in the resulting formulas (Apkarian *et al.* 1995).

Under the natural assumption that the pairs $(A(p), B_2)$ and $(A(p)^T, C_2^T)$ are quadratically stabilizable over the polytope $\mathcal{P}$ (see (Corless 1993) for a definition of quadratic stability/stabilizability) we seek a controller that establishes quadratic $\mathcal{H}_\infty$ performance for the closed-loop system. In particular, we are interested in LPV controllers, that is, controllers with state space representation

$$\Omega(p) := \begin{pmatrix} A_K(p) & B_K(p) \\ C_K(p) & D_K(p) \end{pmatrix} \tag{17}$$

where A_K,B_K,C_K,D_K are affine in a parameter p, which guarantee global stability and $\mathcal{L}_2$-gain of the map from w to z less than γ, such that,

$$\|z\|_2 < \gamma \|w\|_2 \tag{18}$$

for all possible parameter trajectories $p(t) \in \mathcal{P}$. Such a self-scheduled LPV controller is given by the algorithm described in (Apkarian *et al.* 1995).

Numerical Results

The system model (14) was further refined with the addition of weighting functions. The selection of proper weighting functions is an important part of the LPV controller design process.

These weights were chosen so as to penalize excessive shaft displacement, the transmission of forces to the frame, and excessive control effort.

It should be noted that the performance requirements for force attenuation and minimal displacement are conflicting. In order to attenuate imbalance forces, we must allow the rotor to primarily revolve about its inertial axis. This results in fairly large measured displacements at the bearings, which we have also penalized. Omitting the force penalty and concentrating on eliminating displacement results in the rotor being forced to rotate about its geometric axis at the expense of forces transmitted to the frame. On the other hand, penalizing force and ignoring displacement may result in displacements exceeding the clearance spaces at the bearings. Without some penalty on displacement, the controller will not keep the rotor centered in the bearings, and will have poor performance in rejecting steady (DC) loads.

We apply weights to both the force and displacement outputs, thereby characterizing their respective importance. In doing so, we essentially tell the controller how to divide a given amount of imbalance force between rotation about the inertial axis and transmission to the frame. Furthermore, for a given set of weights, we determine how much imbalance the system can handle before the allowable clearance is exceeded. As we increase the displacement penalty relative to the force penalty, we allow for greater imbalances before violating the gap space. In doing so, however, we reduce the force attenuation achieved for all imbalances. Conversely, a high penalty on force relative to displacement gives very good imbalance attenuation, but sacrifices robustness to non-synchronous disturbances, and limits the amount of imbalance that can be tolerated without exceeding available clearance space.

The choice of the force and displacement weights, then, is best done by an iterative process of controller computation and simulation. One reasonable approach would be to design for a certain maximum expected imbalance, and adjust the relative weights so that the controller uses the nearly full clearance to handle this level of imbalance. An acceptable clearance would therefore be maintained for all magnitudes of imbalance below this expected maximum.

Another important question is how to handle the flexible modes of the rotor. The simplest approach would be to ignore them altogether and limit the controller bandwidth to avoid exciting them. This essentially amounts to taking a controller derived for a rigid shaft and implementing it to a flexible system, hoping for the best. Two potential problems exist with this approach, however. First, simply limiting the bandwidth of the controller gives no guarantee that higher frequency flexible modes will not be excited (Balas 1982). Secondly, if we omit the high frequency modes from the model, the controller may have difficulties if these flexible modes show up in the sensor signals. An alternative is to model the high frequency dynamics, but to penalize bearing force at high frequencies, preventing it from exciting these modes. This also prevents a high frequency rotor vibration from being transmitted to the frame of the system. It is this approach that is used here. A potential drawback to this method is the fact that it is vulnerable to errors in the flexible model of the rotor.

The filters chosen for this system were limited by the desire to keep the controller order reasonable. This allows for faster computation, faster simulations, and avoids the difficulty of optimizing the filters in the presence of an excessive number of free variables. It also leads to a quicker computation time, with respect to eventual implementation. After some trial and error, the four force signals were multiplied by the shaping filter $W_f = (s/1000+1)(s/10000+1)$. The displacement output filter W_d is just a multiplication by a gain of 100. This counteracts the tendency of automatic balancing controllers to let the rotor move about freely, and improves the response of the controller to non-synchronous disturbances, as mentioned earlier. The control forces are given a relative weighting of unity, without any dynamics.

A single LPV controller was then designed for operating speeds between 104 and 832 rad/sec (1000 and 8000 rpm). Controller synthesis and testing were performed using `LMITOOLBOX` of `MATLAB` (Gahinet *et al.* 1995) and `SIMULINK`. The γ reported by the LPV controller synthesis program was 545. For comparison purposes, a set of eight single speed $\mathcal{H}_\infty$ controllers were also developed using the same weighting functions, at speeds of 104, 208, 312, 416, 520, 624, 728, and 832 rad/sec. These $\mathcal{H}_\infty$ controllers are measures of the best possible performance at their given operating speeds.

The closed loop γ's for the eight $\mathcal{H}_\infty$ and one LPV controllers are shown in Fig. 2. The asterisks show the achieved performance of the eight $\mathcal{H}_\infty$ controllers at their design speeds. The dashed line is an estimate of the performance that would be achieved by additional $\mathcal{H}_\infty$ controllers at other speeds.

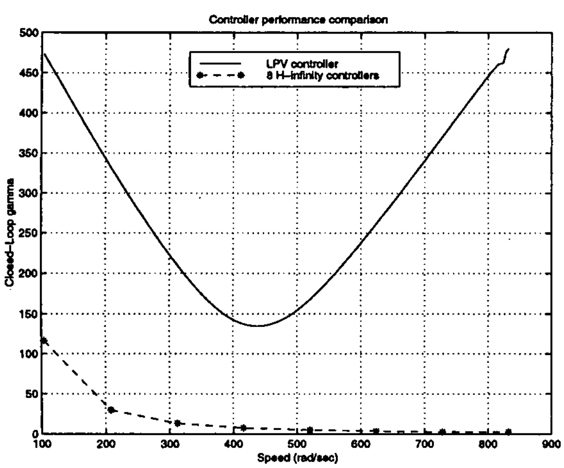

Figure 2: $\mathcal{H}_\infty$ vs. LPV performance

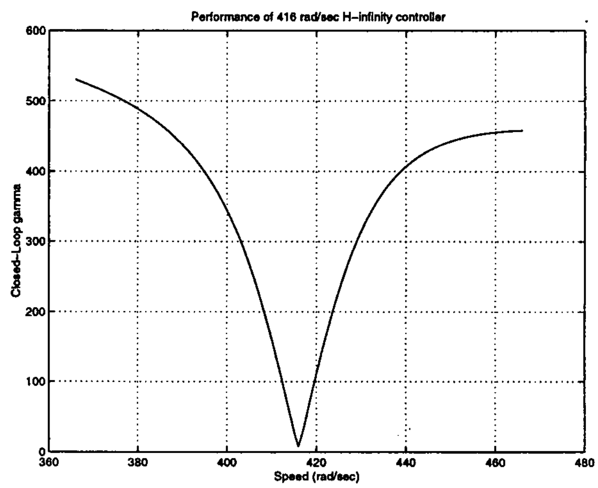

Figure 3: Single speed $\mathcal{H}_\infty$ controller operated over a range of speeds.

These results show that the LPV controller is excessively conservative. Its performance is significantly worse than that of the $\mathcal{H}_\infty$ controllers. However, the $\mathcal{H}_\infty$ controllers are overly optimized for one particular speed, and have poor performance when operating away from the design speed. To ensure that the relative scaling of these performance measures was reasonable, a single speed $\mathcal{H}_\infty$ controller was computed for the center speed 468 rad/sec, and a γ of 6.13 was computed. This is shown in Fig. 3, where the closed loop γ of the 416 rad/sec controller is plotted for operation between 366-466 rad/sec.

The fact that the $\mathcal{H}_\infty$ controller performance drops off rapidly at speeds away from their design speed is due to the fact that an $\mathcal{H}_\infty$ controller is tuned to the particular synchronous disturbance at the rotor speed p and performs poorly when the speed of the rotor is different than the design speed.

Time transient simulations of the $\mathcal{H}_\infty$ and LPV controllers were run at eight different speeds. The results for $p = 520$ rad/sec are shown in Figs. 4-5. Figure 4 shows the response of the LPV controller. The upper plots show the displacements in the X and Y direction at the lower and the upper bearings, respectively. The lower plots show the X and Y components of the force at the lower and upper bearings. Figure 5 shows the corresponding results for the $\mathcal{H}_\infty$ controller. The results for other speeds were similar.

The applied synchronous imbalance force for all cases was 1 lb. Both controllers stabilize the system over all speeds, but the $\mathcal{H}_\infty$ controller achieves better performance in terms of force attenuation. This is expected, since the simulations were run at the design speeds of the $\mathcal{H}_\infty$

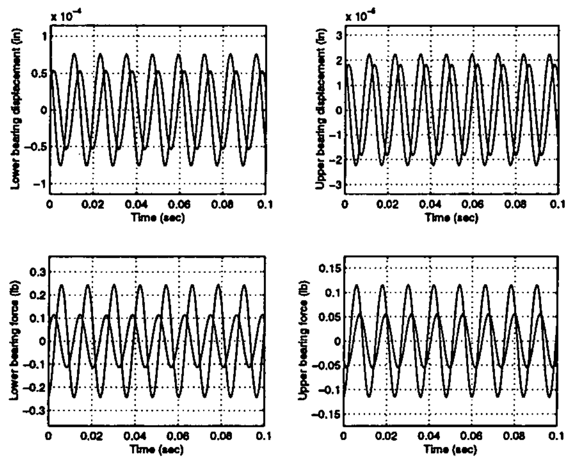

Figure 4: LPV controller response at 520 rad/sec.

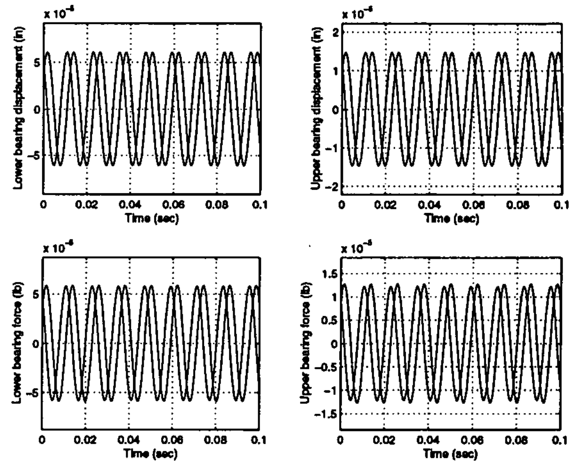

Figure 5: $\mathcal{H}_\infty$ controller response at 520 rad/sec.

controllers, which correspond to the notches in Fig. 8. The performance of both controllers agrees with what is expected from their computed closed-loop γ's. The $\mathcal{H}_\infty$ controller force attenuation and displacement improve with increasing speed. The LPV controller achieves its best performance at 416 rad/sec and 520 rad/sec, speeds corresponding to the bottom of the V-shape in Fig. 8. Force attenuation at these speeds is roughly 80% for the lower bearing and 90% for the upper bearing. The maximum closed-loop γ's for the LPV controller were computed at the vertex speeds 104 rad/sec and 832 rad/sec. As expected, the LPV controller exhibits the worst performance at these speeds, achieving only 50% and 75% force attenuation at the lower and upper bearings, respectively.

Both controllers have higher forces and displacements at the lower bearing than at the upper bearing. This is because the system is non-symmetric. Imbalance forces are being imposed at a point which is closer to the lower bearing than to the upper one. It should also be noted that the displacements of the LPV and $\mathcal{H}_\infty$ controllers are well within the clearance of 0.015 in. It would therefore be possible to obtain improved force attenuation by relaxing the displacement penalty somewhat. For real systems, the tradeoff between force attenuation and displacement would be based on being able to handle a certain maximum expected imbalance without exceeding the clearance space.

Interpolating $\mathcal{H}_\infty$ controllers

In the previous section, we compared the performance of the LPV controller with $\mathcal{H}_\infty$ controllers designed for a single speed. Since we are designing a controller for the entire operating range, this comparison is not fair since the performance of the single-speed $\mathcal{H}_\infty$ controllers does not take into consideration the dynamic effects during the transition from one speed to another. A more fair comparison would be to compute performance for all speeds, not just those for which the $\mathcal{H}_\infty$ controllers were designed. This requires some sort of switching algorithm for the $\mathcal{H}_\infty$ controllers, to compute control outputs at speeds away from the design speeds. Interpolating between the controller matrices themselves is not recommended; doing so assumes a certain consistent structure that a given set of optimal $\mathcal{H}_\infty$ will generally not possess (Hyde 1995). The motivation for the approach used here is the fact that abruptly switching between controllers at set cross over points introduces abrupt changes in the controller output, which should be avoided.

The performance of the LPV and $\mathcal{H}_\infty$ controllers with changing speed was also investigated. Instead of interpolating the controller matrices themselves, as with LPV control, we interpolate the outputs of the two controllers whose design speed is nearest the current operating speed. For a given speed p, the output of the controller is the sum of the lower and higher speed controllers, with their outputs weighted by l and h, respectively. The gains l and h are determined from the rations of actual operating speed and the design speeds of the controllers. This approach does not significantly improve the "preferred speed" nature of the $\mathcal{H}_\infty$ controllers, but it does prevent sudden changes in the controller output.

Two simulations were run, one between 104 rad/sec and 208 rad/sec, and one between 416 rad/sec and 520 rad/sec. In each case the rotor was held at the lower speed for 0.5 sec, accelerated at 250 rad/sec for 4 sec, and then held at the highest speed for 0.5 sec. The results for the second case are shown in Figs. 6-7. The LPV controller achieves better disturbance attenuation than the interpolating $\mathcal{H}_\infty$ controller during the speed-varying portion of the test. This is because the interpolating $\mathcal{H}_\infty$ controller moves away from its design speeds. The performance of the interpolating controller exceeds that of the LPV controller at the start and stop of the simulation, however. This is because the speed trajectory begins and ends at design speeds of the interpolating controller, corresponding to the notches in Fig. 8.

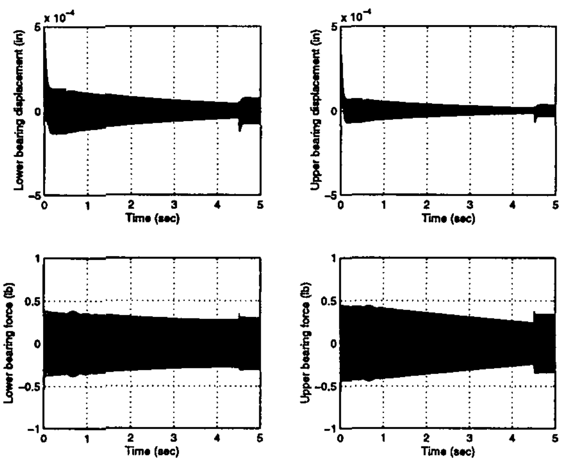

Figure 6: LPV controller response, 416-520 rad/sec.

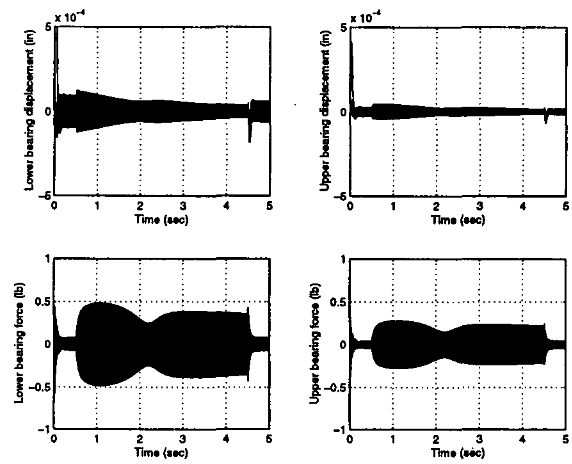

Figure 7: Interpolating $\mathcal{H}_\infty$ controller response, 416-520 rad/sec.

The closed loop γ's for this interpolated $\mathcal{H}_\infty$ approach are shown in Fig. 8, with the LPV γ's included for comparison. As expected, the $\mathcal{H}_\infty$ controller shows a severe drop in performance when operated at speeds away from the 8 design speeds. This could be improved by using a greater number of controllers. Ultimately, an infinite number of controllers would yield performance shown by the dashed line in Fig. 2. This approach is obviously impossible to implement, and would still suffer a loss of performance in the presence of parameter measurement errors. It does, however, provide an absolute benchmark against which to measure alternative approaches such as the LPV controller.

The highly conservative nature of the LPV controller is due in part to the need for a single Lyapunov matrix which shows stability for all parameter values (Apkarian *et al.* 1995). If one can construct a parameter-dependent Lyapunov matrix, an increase in performance would be likely (Tsiotras and Knospe 1997, Apkarian and Adams 1997). To examine this possibility more

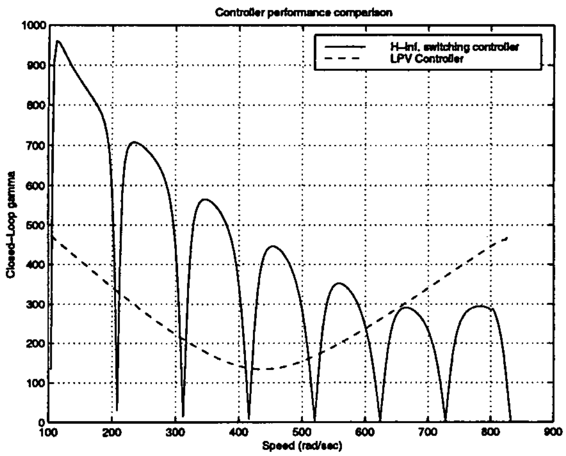

Figure 8: $\mathcal{H}_\infty$ and LPV controller performance.

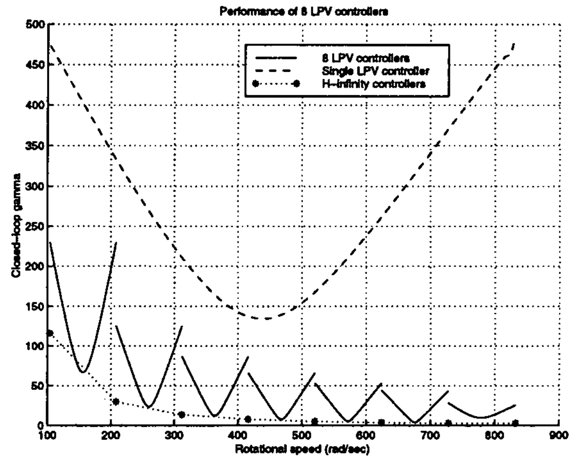

Figure 9: Performance of narrow band LPV controllers.

closely, a set of seven LPV controllers was developed, each covering a 1000 RPM operating range. The closed-loop γ's of the resulting systems are shown in Fig. 9. Again, the single LPV controller and the eight $\mathcal{H}_\infty$ controllers are shown for comparison purposes. As expected, the achieved performance of the individual narrow-band LPV controllers is better than that of the single LPV controller for a given speed range. As with the single LPV controller, the performance of the seven narrow-band controllers is best at the middle speed. Also, the performance of the narrow band LPV controllers approaches that of the optimal, $\mathcal{H}_\infty$ single speed controllers at their midpoint.

Conclusions

We have designed and numerically tested LPV controllers for a flexible rotor with gyroscopics and imbalance forces. The preliminary results show that stability was achieved throughout the operating range and imbalance forces were attenuated. The performance, however, is worse than that of a single speed, $\mathcal{H}_\infty$ controller at the same speed. These $\mathcal{H}_\infty$ controllers, however, cannot be used at speeds that differ greatly from the design speed, as performance quickly deteriorates. Future work should address the derivation of LPV controllers which parameter-dependent Lyapunov matrix solutions in order to improve performance, as well as robustness issues.

ACKNOWLEDGEMENT

This work was partially supported by a grant from American Flywheel Systems, Inc.

References

Ahrens, M., Kucera, L. and Larsonneur, R., 1996, "Performance of a Magnetically Suspended Flywheel Energy Storage Device," IEEE Transactions on Control Systems Technology, Vol. 4, no. 5, pp. 494–501.

Apkarian, P. and Adams, R. J., 1997, "Advanced Gain-Scheduling Techniques for Uncertain Systems," IEEE Transactions on Control Systems Technology, Vol. 6, no. 1, pp. 21–32.

Apkarian, P. and Gahinet, P., 1995, "A Convex Characterization of Gain-Scheduled $\mathcal{H}_\infty$ Controllers," IEEE Transactions on Automatic Control, Vol. 40, no. 5, pp. 853–864.

Apkarian, P., Gahinet, P. and Becker, G., 1994 "Self-Scheduled $\mathcal{H}_\infty$ Control of Linear Parameter-Varying Systems," In: *Proceedings of the American Control Conference* pp. 856–860. Baltimore, MD.

Apkarian, P., Gahinet, P. and Becker, G., 1995, "Self-Scheduled H_∞ Control of Linear Parameter-Varying Systems: a Design Example," Automatica, Vol. 31, no. 9, pp. 1251–1261.

Balas, M. J., 1982, "Trends in Large Space Structure Control Theory: Fondest Hopes, Wildest Dreams," IEEE Transactions on Automatic Control, Vol. 27 pp. 522–535.

Corless, M., 1993 "Robust Stability Analysis and Controller Design with Quadratic Lyapunov Functions," In: *Variable Structure and Lyapunov Control* (A. Zinober, Ed.). Springer-Verlag.

Gahinet, P., Nemirovskii, A., Laub, A. and Chiladi, M. ,1995 LMI Control Toolbox The Mathworks, Inc.

Hyde, R.A., 1995, $\mathcal{H}_\infty$ Aerospace Control Design: VSTOL Flight Application Springer-Verlag London.

Maslen, E. H. and Allaire, P. E., 1991 Magnetic Bearing Synthesis for Rotating Machinery PhD thesis University of Virginia.

Mason, S., 1997 "Linear Parameter Varying Controllers for Magnetic Bearings," Master's thesis University of Virginia Charlottesville, Virginia.

Matsumura, F., Namerikawa, T., Hagiwara, K. and Fujita, M., 1996, "Application of Gain Scheduled $\mathcal{H}_\infty$ Robust Controllers to a Magnetic Bearing," IEEE Transactions on Control Systems Technology, Vol. 4, no. 5, pp. 484–492.

Nonami, K. and Ito, T., 1996, "μ Synthesis of Flexible Rotor-Magnetice Bearing Systems," IEEE Transactions on Control Systems Technology, Vol. 4, no. 5, pp. 503–512.

Packard, Andy, 1994, "Gain Scheduling via Linear Fractional Transformations," Systems and Control Letters, Vol. 22 pp. 79–92.

Sivrioglu, S. and Nonami, K., 1996 "LMI Approach to Gain Scheduled $\mathcal{H}_\infty$ Control Beyond PID Control for Gyroscopic Rotor-Magnetic Bearing Systems," In: *Proceedings of the 35th Conference on Decision and Control* pp. 3694–3699. Kobe, Japan.

Tsiotras, P. and Knospe, C. R., 1997 "Reducing Conservatism for Gain-Scheduled $\mathcal{H}_\infty$ Controllers for AMB's," In: *Proceedings of MAG '97 Industrial Conference and Exhibition on Magnetic Bearings* pp. 290–299. Alexandria, VA.